Int. J. Heat Mass Transfer. Vol. 30, No. 1, pp. 143–150, 1987
Printed in Great Britain

0017–9310/87 \$3.00+0.00
Pergamon Journals Ltd.

Analysis of thermal dispersion effect on vertical-plate natural convection in porous media

J. T. HONG and C. L. TIEN
Department of Mechanical Engineering, University of California, Berkeley, CA 94720, U.S.A.

(*Received* 7 *January* 1986 *and in final form* 14 *April* 1986)

Abstract—The effect of transverse thermal dispersion on natural convection from a vertical, heated plate in a porous medium is examined analytically. The results show that due to the better mixing of the thermal dispersion effect, the heat transfer rate is greatly increased. By taking the no-slip boundary effect into account, it is found that the flow has dual-layer structure. For the inner region, the velocity gradient is very large and the viscous resistance due to the presence of the wall is important. For the outer, much wider, region the velocity gradient is rather small and the viscous resistance term can be neglected. A singular perturbation method is employed to get the higher-order corrections due to the inclusion of the no-slip boundary effect.

INTRODUCTION

BUOYANCY-induced flow from a vertical surface in a porous medium was first studied by Cheng and Minkowycz by using Darcy's law [1]. Numerous investigations [2–8] have been conducted to study the various non-Darcian effects for this type of problem. The inertia effect is shown to decrease the heat transfer when the Rayleigh number is increased [2, 3]. The boundary effect, due to the no-slip boundary condition, also results in a smaller Nusselt number, but is less pronounced as the Rayleigh number is increased [4–6]. For packed-sphere systems, the porosity near the wall is higher than in the bulk region [9] causing an increase in velocity near the wall. The heat transfer is then increased due to this wall-channeling effect. When the inertia effect is prevalent, it is suggested by Cheng [7] and Plumb [8] that the thermal dispersion becomes important. Plumb [8] studied this problem with the no-slip boundary effect neglected and showed that the heat transfer is increased by the thermal dispersion. Several experimental works [10–12] were conducted to determine the effective thermal conductivity for forced convection through fluid-saturated, porous media. It is shown that the effective conductivity can be considered as the sum of a stagnant conductivity (due to molecular diffusion) and a dispersion conductivity (due to mechanical dispersion). In addition, radial temperature distributions measured by these researchers revealed a large temperature gradient near the wall while temperature gradients in the core region are comparably much smaller. Since uniform velocity distributions were assumed in these works, no satisfactory explanation can be given for this 'temperature slip' phenomenon near the wall. This can be explained when the no-slip boundary condition is considered as in the present study. Due to the no-slip condition, the dispersion effect near the wall is much reduced. Therefore the thermal resistance is much higher than that in the core region and a large temperature gradient is observed.

The present study investigates the thermal dispersion effect in addition to the no-slip boundary and inertia effects for natural convection flow. Since the boundary effect is restricted in a very small region near the wall, a singular perturbation method is employed to tackle this problem. The results show that due to the combination of no-slip and dispersion effects, the temperature gradient near the wall is increased, while it decreases for most parts of the thermal boundary layer away from the wall. This kind of temperature profile is similar to that of forced convection in a porous medium [11, 12]. It is also shown that the solution obtained by Plumb [8] is the zeroth-order outer solution of the present problem and the corrections to his results by the inclusion of the boundary effect are clearly shown.

FORMULATIONS OF THE PROBLEM

The analysis applies to a flat, vertical plate embedded in an extended body of fluid-saturated porous medium at uniform temperature. By employing the usual boundary-layer and Boussinesq approximations, the governing equations which include the boundary, inertia and thermal dispersion effects can be written as [5]:

$$u = \frac{\partial \psi}{\partial y}, \quad v = -\frac{\partial \psi}{\partial x} \tag{1}$$

$$\frac{\mu_f u}{K} + \rho_f C u^2 = \rho_f g \beta_f (T - T_\infty) + \frac{\mu_f}{\varepsilon}\frac{\partial^2 u}{\partial y^2} \tag{2}$$

$$u\frac{\partial T}{\partial x} + v\frac{\partial T}{\partial y} = \frac{\partial}{\partial y}\left(\alpha_{\text{eff}}\frac{\partial T}{\partial y}\right). \tag{3}$$

NOMENCLATURE

C	inertia coefficient
c_f	fluid specific heat
Da_x	local Darcy number, K/x^2
Ds	dispersion parameter
d	pore or particle diameter
F	inner dimensionless streamfunction
f	outer dimensionless streamfunction
$\hat{Gr}$	modified Grashof number, $g\beta_f(T_w - T_\infty)K^2C/v_f^2$
g	gravitational constant
K	permeability
k_{eff}	effective thermal conductivity
Nu_x	local Nusselt number
$\hat{Ra}_x$	local Darcy–Rayleigh number, $g\beta_f(T_w - T_\infty)Kx/v_f\alpha_{eff}^\circ$
$\hat{Ra}_d$	Darcy–Rayleigh number based on particle diameter, $g\beta_f(T_w - T_\infty)Kd/v_f\alpha_{eff}^\circ$
$\hat{Re}$	inertia Reynolds number, CKu_D/v_f
T	temperature
u	velocity
u_D	Darcy velocity
x	streamwise coordinate
y	cross-stream coordinate.

Greek symbols

α_f	fluid molecular diffusivity
α_{eff}°	stagnant effective thermal diffusivity
α_d	dispersion diffusivity
β_f	fluid thermal expansion coefficient
γ	mechanical dispersion coefficient
η	outer dimensionless cross-stream coordinate
ε	porosity
σ_x	boundary parameter
ζ	inner dimensionless cross-stream coordinate
δ_m	inner momentum boundary-layer thickness, $(K/\varepsilon)^{1/2}$
μ_f	fluid viscosity
v_f	fluid kinetic viscosity
ρ_f	fluid density
Θ	inner dimensionless temperature
θ	outer dimensionless temperature
ψ	streamfunction.

Subscripts

w	evaluated at wall condition
∞	evaluated at infinity.

Superscripts

$'$	differentiation w.r.t. η or ζ for outer and inner variables, respectively.

It should be noted that the energy equation is based on the assumption of local thermal equilibrium. According to the criteria given by Whitaker [11], this assumption should work well when the ratio of the particle or pore size to the characteristic length of the heated plate is much less than the inverse of the particle Darcy–Rayleigh number to the second power, under the assumption that the conductivities of the solid and fluid phases have the same order of magnitude.

The boundary conditions for equations (1) to (3) are

$$u = v = 0, \quad T = T_w \quad \text{at } y = 0 \tag{4}$$

$$u = 0, \quad T \to T_\infty \quad \text{at } y \to \infty \tag{5}$$

where u and v are the velocity components in the x (along the plate) and y (perpendicular to the plate) directions; ψ, T and g are the streamfunction, temperature and gravitational constant; K, C and ε are the permeability, inertia coefficient and porosity of the porous medium; ρ_f, μ_f and β_f are the density, viscosity and thermal expansion coefficient of the fluid; and $\alpha_{eff} = k_{eff}/(\rho_f c_f)$ is the effective thermal diffusivity of the porous media with $\rho_f c_f$ denoting the product of density and specific heat of the fluid and k_{eff} is the effective thermal conductivity. The subscripts w and ∞ denote the conditions at wall and infinity, respectively. Since a homogeneous porous medium is assumed, K, C and ε are all independent of position.

It is suggested that the effective thermal diffusivity of a saturated porous medium can be expressed as [12–15]:

$$\alpha_{eff} = \alpha_{eff}^\circ + \alpha_d \tag{6}$$

where α_{eff}° is the stagnant diffusivity and α_d is the dynamic diffusivity due to mechanical dispersion. From the volume-averaged, continuum representation of a porous medium, it is seen that the macroscopic concept of thermal dispersion is due to the local temperature and velocity deviations [16]. The general form of the dispersion diffusivity α_d has been investigated by several authors; see for example the review articles by Fried and Combarnous [15]. In the present analysis, it is assumed that α_d can be expressed as:

$$\alpha_d = \gamma u d \tag{7}$$

where d is the dimension of the particle or pore diameter, γ is the dispersion coefficient which is a function of the structure of the porous medium. This kind of representation for α_d is also supported by the previous experimental works [12–15].

By incorporating the nondimensional variables listed below

$$f = \frac{\psi}{\alpha^{\circ}_{\text{eff}} \hat{R}a_x^{1/2}}, \quad \theta = \frac{T - T_\infty}{T_w - T_\infty}, \quad \eta = \frac{y}{x}\hat{R}a_x^{1/2} \quad (8)$$

equations (1)–(3) can be written in the following non-dimensional forms

$$\sigma_x^2 f''' - f' - \hat{G}r(f')^2 = -\theta \quad (9)$$

$$(1 + Dsf')\theta'' + (Dsf'' + 0.5f)\theta' = 0 \quad (10)$$

with the following boundary conditions:

$$f = f' = 0, \quad \theta = 1 \quad \text{at } \eta = 0 \quad (11)$$

$$f' \to 0, \quad \theta \to 0 \quad \text{as } \eta \to \infty. \quad (12)$$

The local Darcy–Rayleigh number in equation (8) is defined as

$$\hat{R}a_x = \frac{g\beta_f \Delta T K x}{\nu_f \alpha^{\circ}_{\text{eff}}}$$

and the primes in equations (9)–(12) refer to the differentiation with respect to the local-similarity coordinate η.

Three parameters in equations (9) and (10) which characterize respectively the boundary, inertia and dispersion effects are

boundary parameter $\sigma_x = (\hat{R}a_x Da_x/\varepsilon)^{1/2}$

modified Grashof number $\hat{G}r = \frac{g\beta_f \Delta T K^2 C}{\nu_f^2}$

dispersion parameter $Ds = \gamma \hat{R}a_d$

where $Da_x = K/(x^2)$ is the local Darcy number and $\hat{R}a_d = g\beta_f \Delta T K d/(\nu_f \alpha^{\circ}_{\text{eff}})$ is the Darcy–Rayleigh number based on the pore or particle size, d.

SINGULAR PERTURBATION SOLUTIONS

Hsu and Cheng [4] and Hong *et al.* [5] have pointed out that the boundary parameter σ_x characterizes the ratio of the inner momentum boundary-layer thickness, of order $(K/\varepsilon)^{1/2}$, to the thermal boundary-layer thickness, of order $x/\hat{R}a_x^{1/2}$. For most porous media σ_x is a very small number and its effect is restricted to a thin region near the wall. To obtain a solution for $\sigma_x \to 0$, a singular perturbation technique is needed. It is assumed that the flow consists of two regions. Near the wall there is a thin region of large velocity gradients where the viscous resistance due to the presence of the wall is important. In the remaining, much wider, region the velocity gradients are small compared with those near the wall and the boundary effect can be considered to be negligible. Accordingly, in the inner region, the similarity coordinate is stretched as follows

$$\zeta = \frac{\eta}{\sigma_x}. \quad (13)$$

Inner expansions for f and θ are taken to be

$$f = \sigma_x[F_0(\zeta) + \sigma_x F_1(\zeta) + \sigma_x^2 F_2(\zeta) + \ldots] \quad (14a)$$

$$\theta = \Theta_0(\zeta) + \sigma_x \Theta_1(\zeta) + \sigma_x^2 \Theta_2(\zeta) + \ldots. \quad (14b)$$

The inner variables and expansions are chosen so that to the lowest order, as $\sigma_x \to 0$, the viscous term which accounts for the no-slip boundary effect is retained.

Writing the governing equations (9), (10) in terms of the inner coordinate (13) and expansions (14), and requiring that the equations be satisfied at each level in powers of σ_x, the following systems of equations are obtained:

$$F_0''' - F_0' - \hat{G}rF_0'^2 = -\Theta_0 \quad (15a)$$

$$\Theta_0'' + Ds(F_0'\Theta_0')' = 0 \quad (15b)$$

$$F_1''' - F_1' - 2\hat{G}rF_0'F_1' = -\Theta_1 \quad (16a)$$

$$\Theta_1'' + Ds(F_0'\Theta_1')' + Ds(F_1'\Theta_0')' = 0. \quad (16b)$$

Note that when dispersion effects are neglected the two lowest-order temperature profiles are linear in the inner region. This can be easily seen from equations (15b) and (16b) by setting $Ds = 0$. These linear temperature profiles will be modified by the consideration of the dispersion effect.

In similar fashion, outer expansions are taken to be

$$f = f_0 + \sigma_x f_1 + \sigma_x^2 f_2 + \ldots \quad (17a)$$

$$\theta = \theta_0 + \sigma_x \theta_1 + \sigma_x^2 \theta_2 + \ldots. \quad (17b)$$

Substituting in the same manner as for the inner equations, the following systems of equations are obtained:

$$f_0'' + \hat{G}r(f_0'^2)' - \theta_0 = 0 \quad (18a)$$

$$\theta_0'' + Ds(f_0'\theta_0)' + 0.5f_0\theta_0' = 0 \quad (18b)$$

$$f_1'' + 2\hat{G}r(f_0'f_1') - \theta_1' = 0 \quad (19a)$$

$$\theta_1'' + Ds(f_0'\theta_1')' + Ds(f_1'\theta_0')' + 0.5(f_0\theta_1' + f_1\theta_0') = 0. \quad (19b)$$

Boundary conditions at the surface ($\zeta = 0$) are obtained by substituting the new variable (13) and the expansions (14) into equation (11) to give:

$$\text{at } \zeta = 0: \quad F_i(0) = F_i'(0) = 0 \quad i = 0, 1, 2, \ldots \quad (20a)$$

$$\Theta_0(0) = 1; \quad \Theta_i(0) = 0 \quad i = 1, 2, \ldots. \quad (20b)$$

Likewise, the boundary conditions far from the surface are obtained by substituting the outer expansions (17) into equation (12) to obtain:

$$\text{at } \eta \to \infty: \quad f_i'(\infty) = 0 \quad i = 0, 1, 2, \ldots \quad (21a)$$

$$\theta_i(\infty) = 0 \quad i = 0, 1, 2, \ldots. \quad (21b)$$

The outer ($\zeta \to \infty$) boundary conditions for the inner equations and the inner ($\eta \to 0$) boundary conditions for the outer equations are obtained by matching the inner and outer expansions. The method used here is similar to that described by Van Dyke [17]. The additional boundary conditions obtained according to this matching principle are:

$$\Theta_0'(\infty) = 0, \qquad F_0'(\infty) = f_0'(0) \tag{22a}$$

$$\theta_0(0) = \Theta_0(\infty), \quad f_0(0) = 0 \tag{22b}$$

$$\Theta_1'(\infty) = \theta_0'(0), \quad F_1''(\infty) = f_0''(0) \tag{23a}$$

$$\theta_1(0) = \lim_{\sigma_x \to 0} (\Theta_1(\infty) - \Theta_1'(\infty)\zeta),$$

$$f_1(0) = \lim_{\sigma_x \to 0} (F_0(\infty) - F_0'(\infty)\zeta). \tag{23b}$$

CALCULATION PROCEDURE

Equation (15b) together with boundary conditions (20b) and (22a) can be easily integrated to give

$$\Theta_0 = 1.$$

Therefore, thermal dispersion has no effect on the basic inner temperature profile Θ_0. If this is combined with equation (22b), the inner boundary conditions for the basic outer solutions f_0 and θ_0 become

$$\theta_0(0) = 1, \quad f_0(0) = 0. \tag{24}$$

This together with the boundary conditions (21a) and (21b) provide enough information to obtain the zeroth-order outer solutions f_0 and θ_0 by integrating (18a) and (18b) using a fourth-order Runge–Kutta scheme. Note that these basic outer equations are exactly the same as those studied by Plumb [8]. Therefore, his solutions provide the basic zeroth-order outer solutions for the present problem.

After obtaining the solutions for f_0 and θ_0, the basic zeroth-order inner velocity expansion F_0' can be obtained by integrating equation (15a) with the boundary conditions given by (20a) and (22a). Since $\Theta_0 = 1$, equation (15a) can be rewritten as

$$F_0''' - F_0' - \hat{G}rF_0'^2 + 1 = 0. \tag{25}$$

This and the boundary conditions (20) and (22) are exactly the same type of equations for a forced boundary-layer flow over a plane surface in porous media by employing the Brinkman–Ergun model (Appendix). It is also noted that the dispersion does not influence F_0 through this governing equation (22). The influence seems to be experienced by F_0 through the matching condition (22). However from equation (18a), it is clearly seen that $f_0'(0)$ is independent of Ds. Therefore, no dispersion effect is experienced by F_0.

The first perturbation for the inner temperature profile, Θ_1, can now be obtained by solving (16b) with boundary conditions given by (20b) and (23a). Then integrating once and applying the results $\Theta_0' = 0$, it can be shown

$$\Theta_1'(\zeta) = \frac{[1 + DsF_0'(\infty)]\theta_0'(0)}{1 + DsF_0'(\zeta)}$$

with boundary condition $\Theta_1(0) = 0$. The temperature gradient at the wall is

$$\Theta_1'(0) = [1 + DsF_0'(\infty)]\theta_0'(0) \tag{26}$$

which is an important quantity in determining the heat transfer.

The inner boundary conditions, $f_1(0)$ and $\theta_1(0)$, for the first outer expansions can now be evaluated from (23b). Together with boundary conditions (21), f_1 and θ_1 can be obtained by integrating (19a) and (19b). Afterwards, the first perturbation for the inner velocity profile, F_1', can be obtained by integrating (16a) with boundary conditions (20) and (23).

To get the numerical results for the heat transfer which account for the boundary effect, the second perturbation of the inner temperature gradient at the wall, $\Theta_2'(0)$, is important. However, there is no need to get complete solutions for Θ_2 throughout the inner region since $\Theta_2'(0)$ can be evaluated from the information provided by the lower-order solutions as shown below.

The governing equations for Θ_2 can be obtained in a similar manner as those for Θ_0 and Θ_1. The result is

$$\Theta_2'' + Ds(F_0'\Theta_2')' + Ds(F_1'\Theta_1')' = 0 \tag{27}$$

with boundary conditions given by

$$\Theta_2(0) = 0 \tag{28a}$$

$$\Theta_2'(\infty) = \theta_0''(0)\zeta + \theta_1'(0) \tag{28b}$$

where equation (28b) is obtained by the matching principle.

Equation (27) can be integrated once to give

$$\Theta_2'(\zeta) = \frac{\Theta_2'(0) - DsF_1'(\zeta)\Theta_1'(\zeta)}{1 + DsF_0'(\zeta)}.$$

Evaluating this at $\zeta \to \infty$ and applying the matching boundary condition (28b), two relations can be obtained

$$\frac{-Dsf_0''(0)\theta_0'(0)}{1 + DsF_0'(\infty)} = \theta_0''(0) \tag{29}$$

$$\frac{\Theta_2'(0) - Dsf_1'(0)\theta_0'(0)}{1 + DsF_0'(\infty)} = \theta_1'(0) \tag{30}$$

where the conditions

$$F_1'(\infty) = f_0''(0)\zeta + f_1'(0)$$

$$\Theta_1'(\infty) = \theta_0'(0)$$

from the matching principle have already been used. It is also noted that the relation (29) can also be obtained by evaluating equation (19b) at the wall. Equation (30) when rearranged gives the result, $\Theta_2'(0)$, needed for calculating the heat transfer from the heating plate, i.e.

$$\Theta_2'(0) = [1 + DsF_0'(\infty)]\theta_1'(0) + Dsf_1'(0)\theta_0'(0). \tag{31}$$

RESULTS AND DISCUSSIONS

The numerically calculated variations of the outer velocity (f_0', f_1') and temperature profiles (θ_0, θ_1) are

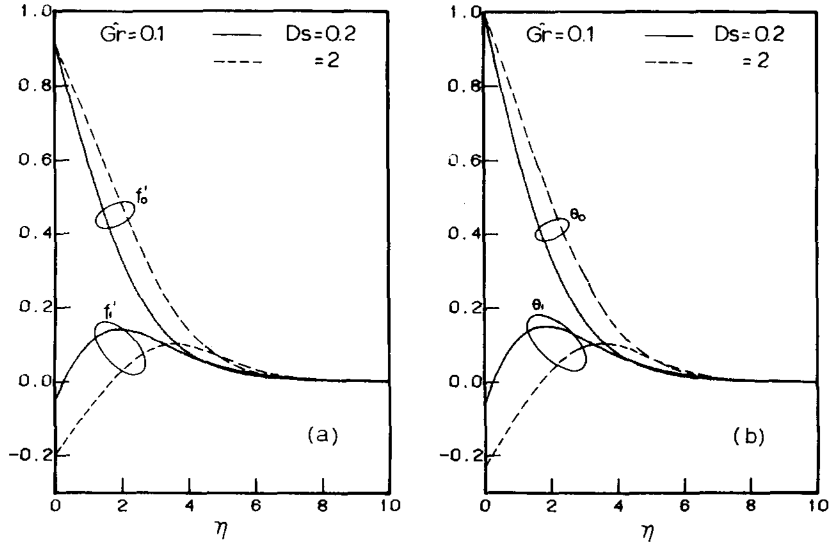

FIG. 1. Perturbation functions of outer expansion: (a) velocity; (b) temperature.

presented in Fig. 1 for $\hat{G}r = 0.1$ and in Fig. 2 for $\hat{G}r = 1$. From these figures it is seen that both inertia and dispersion effects tend to increase the outer boundary-layer thickness. The first-order outer expansions f_1 and θ_1 are negative at $\eta = 0$ when Ds is not zero. This implies that dispersion decreases the velocity and temperature very close to the wall. The magnitude of these negative values increases as Ds becomes larger.

Although the outside profiles f'_0 depend on both the inertia parameter $\hat{G}r$ and the dispersion parameter Ds, $f'_0(0)$ is a function of $\hat{G}r$ only. Then from equation (18a) it is seen that the variations for the zeroth-order velocity expansion F'_0 are independent of the dispersion effect. This is clearly shown in Fig. 3 where F'_0 is shown to be a function of the modified Grashof number only. As discussed earlier, the profiles for F'_0 are similar to those for forced convection boundary layer flows over a flat plate by using the Brinkman–Ergun type of equation. The variations of F'_1 as a function of ζ are presented in Fig. 4 where it is shown that F'_1 is negative and is linear when ζ is large.

Figure 5 shows the results for the first perturbation to the inner temperature. For small Ds the linear profiles indicate that conduction is dominant. For large Ds, Θ_1 is still linear in most portions of the inner region. However, for a very small region near the wall, the profile is no longer linear, and the gradient at the wall is very large. It is concluded that when dispersion effects are important, in a very small region near the wall (smaller than the inner-region thickness), the temperature gradient is greatly increased. As a result,

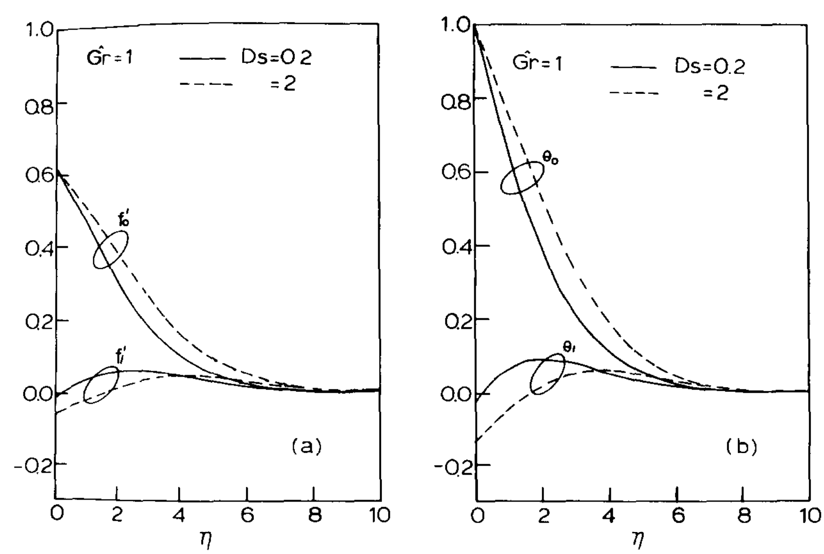

FIG. 2. Perturbation functions of outer expansion: (a) velocity; (b) temperature.

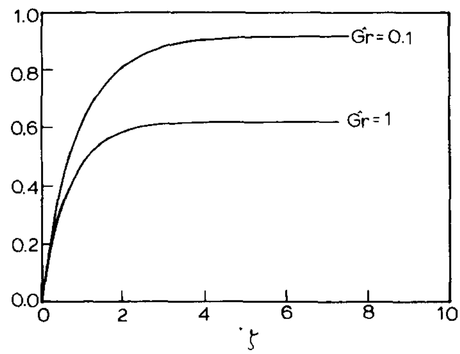

Fig. 3. Zeroth-order inner velocity profiles.

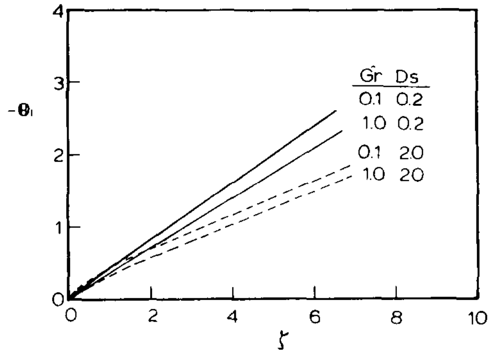

Fig. 5. First-order inner temperature profiles.

the heat transfer is greatly increased due to the dispersion effect. However, in most parts of the thermal boundary layer, the temperature gradient is decreased due to better mixing by the mechanical dispersion effect. This phenomenon is very similar to that for a turbulent flow. In that case, the temperature gradient in most parts of the thermal boundary layer is decreased due to the better mixing by large eddies while the temperature gradient in the viscous sublayer is largely increased.

The most important result to be given is an expression for heat transfer. This can be presented most conveniently by introduction of the local Nusselt number

$$Nu_x = -\frac{x}{(T_w - T_\infty)} \frac{\partial T}{\partial y}\bigg|_{y=0}.$$

By introducing the nondimensional variables, this can be written as

$$\frac{Nu_x}{\hat{R}a_x^{1/2}} = -\frac{1}{\sigma_x} \frac{\partial \theta}{\partial \zeta}\bigg|_{\zeta=0}.$$

From the expansion for the temperature field, the local Nusselt number is related to the gradients $\Theta_1'(0)$ and $\Theta_2'(0)$ at the surface as

$$\frac{Nu_x}{\hat{R}a_x^{1/2}} = -[\Theta'_1(0) + \sigma_x \Theta'_2(0) + \ldots] \quad (32)$$

where $\Theta_1'(0)$ and $\Theta_2'(0)$ are given by equations (26) and (31), respectively.

The calculated values of the temperature derivatives in (32) are listed in Table 1. When both inertia and dispersion effects are neglected ($\hat{G}r = Ds = 0$), the result $\Theta_1'(0)$ is the same as that obtained by Cheng and Minkowycz [1]. The solution $\Theta_2'(0)$ gives a first-order correction due to the inclusion of the boundary effect. Since $\Theta_2'(0)$ is always positive, the boundary effect always decreases the heat transfer. The results for the local Nusselt number according to equation (32) are presented in Table 2. When inertia and dispersion effects are considered, the results show that for large values of the parameter Ds, the dispersion effect dominates and the heat transfer is greatly increased. However, for small values of Ds, the transverse dispersion effect is relatively unimportant and the dominant inertia effect reduces the heat transfer. From the nature of the present analysis, the results given by (32) should be better for smaller values of σ_x. Fortunately, for most porous media, σ_x is very small except for a very short region near the leading edge; therefore, the present analysis should give satisfactory results for most cases. Numerical solutions of the full equations (9) and (10) obtained by using a modified version of the adaptive finite-difference solver (PASVAR) [18] are also presented in Table 2. A comparison of results by these two methods shows that the singular perturbation method gives quite satisfactory results especially for small σ_x. The advantage

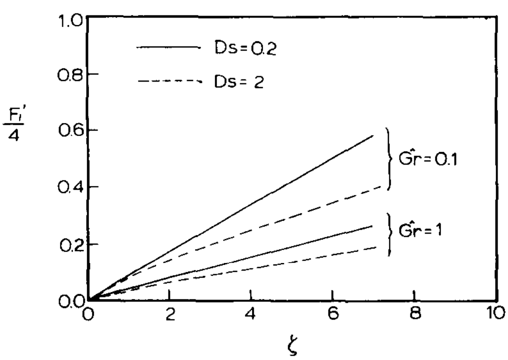

Fig. 4. First-order inner velocity profiles.

Table 1. Solutions for $\Theta_1'(0)$ and $\Theta_2'(0)$

$\hat{G}r$	Ds	$\Theta_1'(0)$	$\Theta_2'(0)$
0	0	−0.4438	0.2945
0.1	0	−0.4295	0.2524
	0.2	−0.4575	0.2938
	2	−0.6574	0.5099
	5	−0.8957	0.6922
1	0	−0.3658	0.1299
	0.2	−0.3827	0.1447
	2	−0.5098	0.2340
	5	−0.6697	0.3199

Table 2. Numerical results for $Nu_x/\hat{R}a_x^{1/2}$

$\hat{G}r$	Ds	σ_x	$Nu_x/\hat{R}a^{1/2}$ Perturbation	Finite difference	Percentage difference
0	0	0.1	−0.414350	−0.417011	0.638
		0.05	−0.429075	−0.429728	0.151
		0.01	−0.440855	−0.440839	0.004
0.1	0.2	0.1	−0.428120	−0.430647	0.587
		0.05	−0.442810	−0.443511	0.158
		0.01	−0.454562	−0.454639	0.018
	2	0.1	−0.606410	−0.610966	0.746
		0.05	−0.631905	−0.633191	0.202
		0.01	−0.652301	−0.652354	0.008
	5	0.1	−0.826480	−0.833694	0.865
		0.05	−0.861090	−0.863571	0.287
		0.01	−0.888778	−0.889109	0.037
1	0.2	0.1	−0.368230	−0.368922	0.187
		0.05	−0.375465	−0.375659	0.051
		0.01	−0.381253	−0.381262	0.003
	2	0.1	−0.486400	−0.487830	0.293
		0.05	−0.498100	−0.498558	0.092
		0.1	−0.507460	−0.507529	0.014
	5	0.1	−0.637710	−0.640359	0.414
		0.05	−0.653705	−0.654710	0.153
		0.01	−0.666501	−0.666659	0.024

of this method over the other one is that it gives results which display the boundary effect explicitly. In addition, it exposes the predominant factors in different parts of the boundary layer.

CONCLUSIONS

The steady natural convection heat transfer from a vertical, isothermal, heated plate in porous media is studied analytically. Three parameters are found to characterize three non-Darcian effects: boundary, inertia and dispersion effects. By the inclusion of the no-slip boundary effect, it is found the flow consists of two distinct regions: an inner region exists near the surface where the velocity gradient is very large and the viscous term cannot be neglected. Away from the wall, a much wider region exists where the boundary effect can be neglected. Using the method of matched asymptotic expansions, it is found that dispersion has no effect on the zeroth-order inner expansions. The zeroth-order inner velocity profile is found to be similar to that for a forced convection boundary layer over a flat surface. Both the inertia and boundary effects are found to decrease the heat transfer, while dispersion will increase the heat transfer. Whether the heat transfer is increased or decreased depends on the relative magnitude of these three mechanisms.

REFERENCES

1. P. Cheng and W. J. Minkowycz, Free convection about a vertical flat plate embedded in a porous medium with application to heat transfer from a dike, *J. geophys. Res.* **82,** 2040–2044 (1977).
2. O. A. Plumb and J. C. Huenefeld, Non-Darcy natural convection from heated surfaces in saturated porous media, *Int. J. Heat Mass Transfer* **24,** 765–768 (1981).
3. A. Bejan and A. Poulikakos, The non-Darcy regime for vertical boundary layer natural convection in a porous medium, *Int. J. Heat Mass Transfer* **27,** 717–722 (1984).
4. C. T. Hsu and P. Cheng, Brinkman's model for free convection about a flat plate in a porous medium, *Int. J. Heat Mass Transfer* **28,** 683–697 (1985).
5. J. T. Hong, Y. Yamada and C. L. Tien, Effects of non-Darcian and non-uniform porosity on vertical-plate natural convection in porous media, *J. Heat Transfer* (in press).
6. J. T. Hong, C. L. Tien and M. Kaviany, Non-Darcian effects on vertical-plate natural convection in porous media with high porosities, *Int. J. Heat Mass Transfer* **28,** 2149–2157 (1985).
7. P. Cheng, Thermal dispersion effects in non-Darcian convective flows in a saturated porous media, *Lett. Heat Mass Transfer* **8,** 267–270 (1981).
8. O. A. Plumb, The effect of thermal dispersion on heat transfer in packed bed boundary layers, *ASME–JSME Joint Thermal Conference Proc.*, Vol. 2, pp. 17–21 (1983).
9. R. F. Benenati and C. B. Brosilow, Void fraction distribution in a bed of spheres, *A.I.Ch.E. Jl* **8,** 359–361 (1962).
10. D. A. Plautz and H. F. Johnstone, Heat and mass transfer in packed beds, *A.I.Ch.E. Jl* **1,** 193 (1955).
11. S. Whitaker, Local thermal equilibrium: an application to packed bed catalytic reactor design, *Chem. Engng Sci.* **41,** 2029–2039 (1986).
12. S. Yagi, D. Kunii and K. Endo, Heat transfer in packed beds through which water is flowing, *Int. J. Heat Mass Transfer* **7,** 333–339 (1964).
13. D. Kunii and M. Suzuki, Heat transfer between wall surface and packed solids, *A.I.Ch.E. Jl* **12,** 344–352 (1966).
14. A. P. De Wasch and G. F. Fremont, Heat transfer in packed beds, *Chem. Engng Sci.* **27,** 567–576 (1972).
15. J. J. Fried and M. A. Combarnous, Dispersion in porous media, *Adv. Hydrosci.* **11,** 169–282 (1976).
16. R. G. Carbonell and S. Whitaker, Heat and mass transfer in porous media, *NATO Advanced Study Institute on the Mechanics of Fluid Flow in Porous Media*, University of Delaware, 18–27 July (1982).
17. M. Van Dyke, *Perturbation Methods in Fluid Mechanics*. Parabolic Press, Stanford, CA (1975).
18. M. Lentini and V. Pereyra, An adaptive finite difference solver for non-linear two-point boundary problems with mild boundary layers, *SIAM J. Numer. Anal.* **14,** 91–111 (1977).

APPENDIX

By employing the well known Brinkman–Ergun model for non-Darcian flow, the governing equation for a forced boundary-layer flow over a plane surface can be written as

$$-\frac{dp}{dx} = \frac{\mu_f u}{K} + \rho_f C u^2 - \frac{\mu_f}{\varepsilon}\frac{d^2 u}{dy^2}$$

with boundary conditions

$$\text{at } y = 0: \quad u = 0$$

$$\text{at } y \to \infty: \quad u \to u_\infty.$$

These equations can be nondimensionalized by using the Darcy velocity u_D and inner momentum boundary-layer thickness δ_m

$$u_D = -\frac{K}{\mu_f}\frac{dp}{dx}, \quad \delta_m = \left(\frac{K}{\varepsilon}\right)^{1/2}.$$

By defining the nondimensional streamfunction, F, the nondimensional coordinate, η, as

$$F = \frac{\psi}{u_D(K/\varepsilon)^{1/2}}, \quad \eta = \frac{y}{(K/\varepsilon)^{1/2}}$$

then

$$u = \frac{d\psi}{dy} = u_D F'$$

and governing equation and the boundary conditions are transformed to

$$F''' - F' - \hat{R}eF'^2 + 1 = 0$$

$$F'(0) = 0, \quad F'(\infty) = \frac{u_\infty}{u_D}$$

where the inertia Reynolds number $\hat{R}e = CKu_D/\nu_f$ is analogous to the modified Grashof number $\hat{G}r$.

ANALYSE DE L'EFFET DE LA DISPERSION THERMIQUE SUR LA CONVECTION NATURELLE DANS UN MILIEU POREUX CONTRE UNE PLAQUE VERTICALE

Résumé—On examine analytiquement l'effet de la dispersion thermique transversale sur la convection naturelle dans un milieu poreux à partir d'une plaque chaude verticale. Les résultats montrent qu'à cause du meilleur mélange par l'effet de dispersion thermique, le flux de chaleur est fortement accru. En prenant en compte la condition de non glissement, on trouve que l'écoulement a une structure de couche duale. Pour la région interne, le gradient de vitesse est très grand et la résistance visqueuse due à la présence de la paroi est importante. Pour la région externe plus épaisse, le gradient de vitesse est plutôt faible et le terme de résistance visqueuse peut être négligé. Une méthode de perturbation singulière est employée pour obtenir des corrections d'ordre élevé dues à l'inclusion de l'effet de frontière sans glissement.

UNTERSUCHUNG DES THERMISCHEN AUSBREITUNGSEFFEKTES AUF EINER VERTIKALEN PLATTE BEI NATÜRLICHER KONVEKTION IN PORÖSEN MEDIEN

Zusammenfassung—Der Einfluß der thermischen Querausbreitung auf die natürliche Konvektion an einer vertikalen geheizten Platte in einem porösen Medium wird analytisch untersucht. Die Ergebnisse zeigen, daß infolge einer verbesserten Vermischung durch den Effekt der thermischen Querausbreitung der Wärmeübergang stark verbessert wird. Zieht man den schlupflosen Grenzschichteffekt in Betracht, zeigt sich eine Zweilagenstruktur der Strömung. Im inneren Bereich ist der Geschwindigkeitsgradient sehr groß und die Reibungskraft wird im Wandbereich dominierend. Im äußeren, viel größeren Strömungsgebiet ist der Geschwindigkeitsgradient recht klein und die Reibungskraft kann vernachlässigt werden. Es wird eine Strömungsmethode zur Ermittlung der Korrekturfaktoren höherer Ordnung herangezogen.

АНАЛИЗ ВЛИЯНИЯ РАСПРОСТРАНЕНИЯ ТЕПЛА НА ЕСТЕСТВЕННУЮ КОНВЕКЦИЮ ОКОЛО ВЕРТИКАЛЬНОЙ ПЛАСТИНЫ В ПОРИСТОЙ СРЕДЕ

Аннотация—Аналитически исследуется влияние поперечного переноса тепла на естестенную конвекцию около вертикальной нагреваемой пластины в пористой среде. Результаты показывают, что, благодаря лучшему перемешиванию, индуцированному распространением тепла, интенсивность теплопереноса значительно растет. В предположении отсутствия скольжения на границе найдено, что течение имеет двухслойную структуру. Для внутренней области градиент скорости очень высок и вязкое сопротивление из-за наличия стенки весьма существенно. Для наружной, более широкой зоны, градиент скорости довольно мал и членом, описывающим вязкое сопротивление, можно пренебречь. Для получения поправок высшего порядка с учетом отсутствия скольжения на стенке применяется метод сингулярных возмущений.